An Annular Resonator Used To Measure the Speed of Sound in Gaseous Fluoroalkanes: Trifluoromethane and Hexafluoroethane

Gary K. Jarvis, Kathleen A. Johnson,* and Susan L. Walmsley

Department of Chemistry, The University of Liverpool, P.O. Box 147, Liverpool L69 3BX, U.K.

A simple annular resonator is presented in which it is possible to measure the speed of sound with an accuracy of about 0.05%. Results are presented for gaseous trifluoromethane at nine temperatures in the range (294 to 318) K and for hexafluoroethane at six temperatures in the range (281 to 321) K. Measurements have been made in the pressure range (1 to 50) bar or 1 bar to 90% of the vapor pressure, which ever is higher. For trifluoromethane, the expected minimum near the critical point has been observed. Both sets of experimental measurements have been compared with the speed of sound predicted by classical equations of state.

1. Introduction

Measurements of the speed of sound are a useful tool to test proposed equations of state or thermodynamic potentials as they are directly related to the curvature of the potential. In a single-phase system, the speed of sound can either increase or decrease with pressure, depending on whether repulsive or attractive forces dominate. Above the critical point this leads to minima in the pressure dependence. As the critical point is approached, the minima become very sharp. Although this behavior is predicted by analytical potentials, it is necessary to employ nonanalytical potentials to obtain the correct shape of the minima.

An annular resonator has previously been used to measure the speed of sound in near-critical xenon (Garland and Williams, 1974). However, the results were not of sufficient precision to establish, unambiguously, the form of the critical dependence. The aim of this work was to attempt to improve the precision of the technique by employing recent developments in both the theoretical understanding and modern electronics. Work, pioneered by Mehl and Moldover (1981), has shown that spherical resonators can be used with relative ease to measure the speed of sound with extremely high precision (Moldover et al., 1988; Ewing et al., 1986). Recent work by Ewing and Trusler (Ewing and Trusler, 1989a; Ewing et al., 1989b; Ewing and Goodwin, 1992; Trusler and Zarani, 1992; Trusler, 1994) has shown that the precision can be maintained over a wide range of temperature and pressure. Spherical resonators have also been used with significant success to obtain information about ideal-gas heat capacities (Ewing and Trusler, 1989; Colgate et al., 1990) and phase transitions of both pure (Colgate et al., 1991a) and multicomponent (Colgate et al., 1991b) systems.

There is, however, a major difficulty in using spherical resonators to measure the speed of sound near the critical state of a fluid. Accurate measurements in the critical region must be made on samples of small height to minimize any gravitational effects, but to obtain small sample heights with a spherical resonator, the radius of the resonator must be minimized. This rapidly increases the resonance frequencies of the radial modes, and so, as it is important to study the low-frequency limit of the speed of sound, a compromise has to be made.

In an attempt to overcome this we have chosen to explore the use of a different geometry. If an annular resonator is chosen, it is possible to study azimuthal resonances (that is, those resonances that go around the ring). For a resonator with a relatively small height (10 mm in this work) and small volume (31×10^3 mm^3), resonances occur at reasonably low frequencies (we use a frequency range of 400 Hz to 10 kHz). Annular resonators have the additional advantage that fabrication is significantly easier, and that the separations of the modes can be "tuned" by altering the ratio of the internal and external radii.

In this paper we present the results of a series of measurements on the speed of sound in fluid trifluoromethane and in fluid hexafluoroethane. The expected minimum in the speed of sound near the critical region has been observed for trifluoromethane, but we have not been able to explore the minimum in the speed of sound for hexafluoroethane. For both fluids the results have been compared with equations of state.

2. Apparatus

The apparatus used to measure the speed of sound can be considered to consist of three parts: the pressure vessel containing the annular resonator, the computer-controlled data acquisition system, and the gas-handling system. In the design of the apparatus, considerable emphasis was placed on ease of fabrication.

2.1. Pressure Vessel and Annular Resonator. The internal diameter is 110 mm, the internal depth 35 mm, and the wall thickness 15 mm. A diagram of the pressure vessel and annular resonator is shown in Figure 1. The vessel (A) was fabricated from a piece of steel rod and is sealed with a simple Viton "O" ring seal (B). It has been designed to work at pressures up to 70 bar. The annular resonator (C) is located inside the pressure vessel by means of four small PTFE "feet" (D). The resonator is fabricated from an aluminium alloy in two parts. The cavity has been machined out of the bottom half by cutting a rectangular channel (11 mm × 10 mm) out of the circular block (diameter 108 mm) at a constant radius (internal radius 45 mm) (E). Two small holes (1 mm diameter) have been drilled through the bottom of the channel to allow access for the fluid contained in the pressure vessel. The upper half (F) acts as a lid to the cavity. It has a lip (1 mm) which locates in the channel, and two holes (180° apart) for the drive (G) and pickup (H) acoustic transducers. The lid is secured to the bottom with four small screws. The drive transducer (piezoelectric, ceramic type) is arranged so that the fluid in the annular cavity sees only a 1 mm diameter

* To whom correspondence should be addressed. E-mail: K.A.Johnson@liverpool.ac.uk.

0021-9568/96/1741-0222$12.00/0

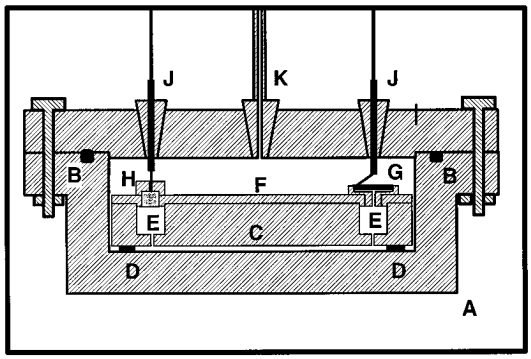

Figure 1. Pressure vessel and annular resonator. The various components, as identified in the text are as follows: (A) pressure vessel; (B) O-ring seal; (C) bottom section of the annular resonator; (D) PTFE feet; (E) annular cavity; (F) lid of the resonator; (G) drive transducer; (H) pick-up transducer; (J) lead-throughs; (K) filling valve.

hole. The pickup transducer (electret microphone) is located flush with the inside of the lid. The top of the pressure vessel contains all the necessary electrical lead-throughs (J), a stainless-steel valve for filling (K), and a differential pressure transducer (not shown in the diagram). The pressure transducer is designed to measure the difference in pressure between the fluid in the pressure vessel and that in a reference line with a precision of ±0.3 kPa.

The pressure vessel is suspended from the lid of an outer copper jacket which provides a water-tight cavity for the vessel, the pressure transducer, and the associated electronics. The leads and filling tubes are taken out of the thermostat using brass pipes. The valve, which is also located within the water jacket, can be opened and closed using a brass extension handle. Finally, a stirred-water bath is used as a thermostat, the temperature of which is kept constant to better than ±0.001 K. The temperature of the bath is measured using a standard platinum resistance thermometer which has been calibrated against IPTS-68. The resistance of this thermometer and a small platinum resistance thermometer inside the pressure vessel is measured using an automatic temperature bridge. This bridge can be read by the computer when required.

2.2. Data Acquisition System. The speed of sound of the fluid contained in the pressure vessel is determined by measuring the frequencies of the azimuthal resonances in the cavity. The drive transducer is driven directly by a precision frequency synthesizer; no further amplification is needed. The in-phase and out-of-phase voltages of the signal received at the pickup transducer are measured using a lock-in amplifier. Once the rough location of the resonance has been determined manually, the exact location is established by measuring the received signal at approximately 11 frequencies in the range ($f_r - g$) to ($f_r + g$), where f_r is the frequency of the resonance and g is its half-width. This process is controlled by a personal computer with the aid of an IEEE-488 interface. The pressure difference measured on the pressure transducer, the temperature of the water bath, and the temperature inside the pressure vessel are read at the same time. In most cases all of the observable peaks in the range (1 to 10) kHz are measured. The resonance frequencies (f_0) and half-widths (g_0) are determined by representing the measured in-phase (u) and out-of-phase (v) voltages by an equation of the form

$$u + iv = iAf/(f_0 + ig_0) - B - Cf \qquad (1)$$

where f is the measured frequency and A, B, and C are complex constants, using a nonlinear fitting technique. In many cases it was not necessary to include the frequency dependence of the background (that is, the term in C).

2.3. Gas-Handling System. The gas-handling system consists of two parts: the reference side and the sample side. The filling procedure for gases such as CHF_3 and C_2F_6 is straightforward; enough gas is transferred from the supply cylinder to a sample cylinder to complete a run, and is degassed. Sufficient fluid is then transferred to the pressure vessel to obtain the required pressure, the pressure vessel is isolated, and a set of resonances is measured. A new pressure is then obtained by adding more fluid from the sample cylinder. The difference between the pressure of the vessel and that of the reference side is measured using the differential pressure transducer. Since this can measure differences up to 12 bar, the amount of reference gas is adjusted so that the pressure difference falls within this range. The absolute pressure is measured using one of two Budenburg gauges (standard test gauge; (0 to 10) bar gauge or (0 to 40) bar gauge). The gauges enable us to measure pressure with an accuracy of ±0.05 bar for pressures above 10 bar, and ±0.01 bar for pressures below 10 bar.

Most of the development work has been performed using argon. The apparatus was tested at a range of temperatures and pressures to test the feasibility of the design. Measurements at low pressure lead to a value of the internal radius of the resonator. However, as the apparatus has not been designed to make accurate measurements at low pressure, we were not able to improve on the precision of a mechanical measurement (about 0.1%). Mechanical measurement gave the external radius a of the annulus to be 0.04500 m and the radius ratio b/a to be 0.7791. Within the precision of this experiment, the variation of a and b/a with temperature was insignificant. Any variation with pressure would be minimized as this was the same inside and outside of the resonator.

3. Theory

To find the frequencies of the resonances of an annular-shaped cavity, it is necessary to find the solutions of the wave equation for a cavity of this geometry. The wave equation can be solved using standard techniques, the only complication being that the correct form of the radial part of the solution must include both the Bessel and the Neumann functions as the origin of the system is not part of the cavity. Solutions of the wave equation are described in terms of eigenvalues found by applying suitable boundary conditions. To a first approximation, the boundary conditions for the azimuthal modes are

$$dF(r)/dr = 0 \text{ at } r = a \text{ and } r = b$$

where $F(r)$ is the radial part of the solution of the wave function, a is the outer radius of the annulus, and b is the inner radius. In terms of Bessel (J_m) and Neumann (N_m) functions, the equivalent equation is

$$J_m'(\chi_{mn})/N_m'(\chi_{mn}) = J_m'(\chi_{mn}b/a)/N_m'(\chi_{mn}b/a)$$

where the prime refers to the differential of the function with respect to r (Morse and Ingard, 1968). Solution of this equation leads to discreet values of the eigenvalue χ_{mn} that depend on the radius ratio b/a. The lowest frequency azimuthal resonances are given by the solutions with $n = 0$ and $m = 1, 2, \ldots$. For our resonator these modes are approximately equally spaced, and start at about 1.3 kHz for argon at atmospheric pressure. Azimuthal modes with $n > 0$ and longitudinal modes all occur at frequencies above

Table 1. Allowed Values of the Eigenvalue χ_{m0} for a Radius Ratio b/a of 0.7791

m	χ_{m0}	m	χ_{m0}	m	χ_{m0}
1	1.126 975	2	2.253 516	3	3.379 193
4	4.503 575	5	5.626 239	6	6.746 772
7	7.864 768	8	8.979 841	9	10.091 626
10	11.199 784	11	12.304 013	12	13.404 053
13	14.499 691	14	15.590 771	15	16.677 196

16 kHz. Table 1 gives values of χ_{m0} for $m = 1-15$, assuming $b/a = 0.7791$. An uncertainty of 1% in b/a leads to an uncertainty of 0.4% in χ_{m0}.

To relate the observed frequency (f) of the resonance to the eigenvalue (χ_{mn}) of the mode and hence to the speed of sound (u) requires a knowledge of the behavior of the walls of the resonator and of the fluid under study. If, to a first approximation, we assume that the walls of the resonator are perfectly rigid and that the effects of thermal and viscous damping in the fluid are negligible, we can say that

$$u/a = 2\pi f/\chi_{mn} \qquad (2)$$

This approximation is also inherent in our solutions of the wave equation (Morse and Ingard, 1968).

To proceed further, we must account for various loss mechanisms in the resonator. The most difficult is the loss due to viscous damping at the walls of the resonator. This depends on the tangential motion of the fluid at the walls. Work with a spherical resonator eliminates this problem (Mehl and Moldover, 1981) as, if the radial modes of the sphere are chosen, there are no tangential losses. Unfortunately, for the azimuthal modes of an annulus, the problem is far from simple, as the tangential component varies with θ. In this work we have chosen to follow a slightly simpler approach. In an attempt to allow for the loss mechanisms, we assume that all losses except those due to bulk viscosity, bulk thermal conductivity, and molecular relaxation contribute equally to the width of the observed peak and to a reduction in the frequency of the resonance. Hence, we measure the width of the peak g_0 as well as the frequency of it maximum f_0 (via eq 1), subtract the contributions due to the bulk of the fluid g_b from g_0, and add the result to f_0. The resulting frequency is then used in eq 2 to calculate u/a. We believe that any errors in this procedure are less than the uncertainty in our measurements, and so the additional complication of obtaining the exact solution for the losses in our cavity is not necessary.

4. Materials

The trifluoromethane (R23) was supplied by BOC (electra grade) and was stated to be 99.998% pure. The hexafluoroethane (R116) was supplied by Fluorochem and was stated to be 99.9% pure. Immediately before use both gases were degassed by repeatedly freezing the fluid, pumping it onto the solid, and thawing the solid, until there was no observable change in pressure. No analysis or further purification was attempted. The argon used in the experiments was also supplied by BOC and had a stated purity of 99.9%.

5. Results

Resonance frequencies and half-widths were measured for between five and seven azimuthal modes of the cavity over a range of pressures at the temperatures of interest. At each temperature a set of measurements was made for argon as well as the fluoroalkane. The quality factors of the resonances ($Q = f/2g$) were much smaller than those observed in spherical resonators (ranging from about 150 to 500 as opposed to between 4000 and 30 000), and so the precision of the measurements was necessarily much lower. However, over most of the density range the precision in g was between 0.2% and 0.4%, leading to an uncertainty in f of less that 0.01%.

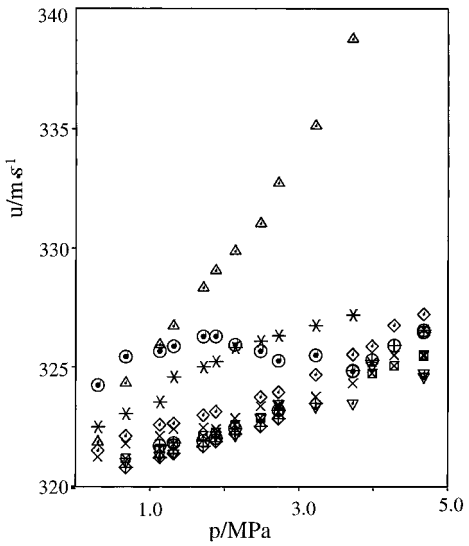

Figure 2. Speed of sound u in argon at 296.85 K as a function of pressure p, as given by the first nine modes of the resonator: (△) $m = 1$; (⊙) $m = 2$, (*) $m = 3$; (dotted tilted square) $m = 4$; (×) $m = 5$; (⊕) $m = 6$; (× inside square) $m = 7$; (+ inside tilted square) $m = 8$; (dotted inverted triangle) $m = 9$. There is significant coupling between the motion of the fluid and that of the shell for the first three modes.

As an illustration of the precision of our measurements, results for argon at 296.85 K are plotted in Figure 2. The speed of sound for each resonance is plotted as a function of pressure. This set of results is typical of all the measurements made in the resonator. The variation of the speed of sound with pressure for the first three resonances suggests that there is significant coupling between the shell and the fluid at low frequencies. For resonances at higher frequencies the coupling appears to disappear, and an average of the fourth, fifth, sixth, seventh, eighth, and ninth peaks appears to be a good estimate of the measured speed of sound in argon. For all of the measurements in argon, we have used the average of these six peaks. To ascertain the precision of our measurements, we have represented the speed of sound for each isotherm by a polynomial in pressure. Figure 3 shows the results of this analysis for the isotherm at 296.85 K. For a fit to a quadratic equation the standard error of the fit was 0.135 m s^{-1}, indicating a precision of better than 0.05%.

To ascertain the accuracy of our measurements, we have compared our measurements with the excellent results obtained by Ewing and Goodwin (1992) in a spherical resonator. Figure 3b compares the differences between our measurements and those of Ewing interpolated to 296.85 K and (0 to 5) MPa (squares) and the residual from our fit to a quadratic equation (circles). Although the deviations of our measurements from those obtained by Ewing et al. are greater than our residuals from our best fit, the difference is not great and shows few signs of any systematic error. Similar results were obtained at all of the temperatures studied in this paper. This indicates that it is fair to conclude that our resonator is capable of producing measurements of the speed of sound that are accurate to better than 0.05%.

5.1. Results for Trifluoromethane. The results obtained for a particular state ($T = 299.551$ K, $p = 2.098$ MPa) of the system are illustrated in Table 2. The in-phase and

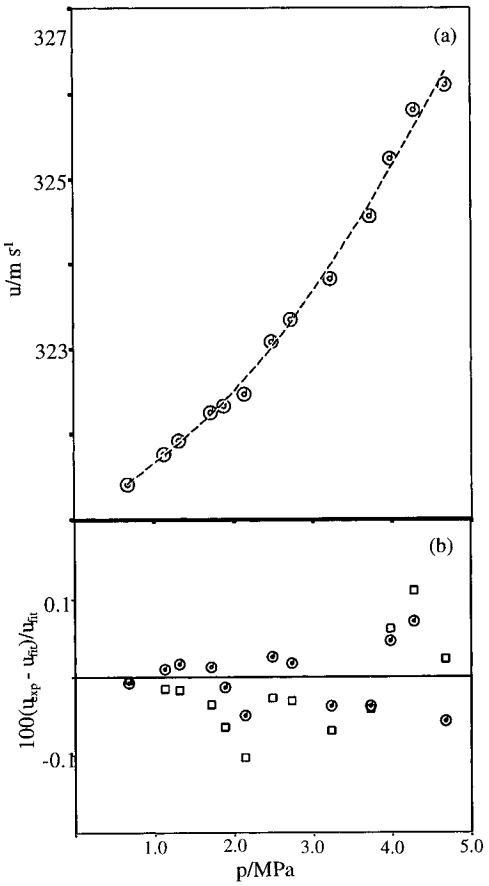

Figure 3. Average speed of sound u in argon at 296.85 K. The average speed of sound was found by taking an unweighted average of the fourth, fifth, sixth, seventh, eighth, and ninth resonances. (a) The circles indicate the experimental measurements, and the dashed line represents the line of the best fit. (b) The circles represent the percentage deviation of the experimental measurements from the line of the best fit, and the squares represent the percentage deviation of the experimental measurements from previous measurements in a spherical resonator (Ewing et al., 1992).

Table 2. A Typical Series of Resonances, T = 299.551 K, p = 2.098 MPa[a]

m	f_0/Hz	g_0/Hz	g_b/Hz	$(u/a)^b$/Hz = $[2\pi(f_0 + g_0 - g_b)]\chi_{m0}$]/Hz	$\sigma^c(u/a)$/Hz
5	3623.51	7.83	0.58	4054.70	0.53
6	4346.37	6.87	0.83	4053.34	0.03
7	5067.14	7.38	1.13	4053.15	0.16
8	5785.94	7.86	1.47	4052.88	0.09
9	6500.80	7.98	1.86	4051.30	0.05
10	7215.90	9.05	2.30	4051.42	0.06
11	7930.21	9.89	2.77	4053.29	0.12
12	8644.33	7.85	3.30	4054.19	0.20

[a] The measured frequencies and voltages for each resonance have been represented by eq 1 and estimates of the frequency of the peak maximum (f_0) and the peak half-width (g_0) obtained. The measured half-width has been corrected for losses due to bulk absorption (g_b) before being used to obtain a value for the ratio u/a, where u is the speed of sound and a the external radius of the annulus. [b] Unweighted mean (4053.03 ± 0.42) (the quoted uncertainty is the standard error of the mean). [c] $\sigma(u/a)$ is an estimate of the uncertainty in u/a obtained from the uncertainties in f_0 and g_0 given by the nonlinear fitting program.

out-of-phase voltages were measured at 21 frequencies surrounding each resonance. It soon became clear that, for the lower speeds of sound observed in trifluoromethane, it was necessary to reject the first four resonances due to coupling between the fluid and the shell. The results for

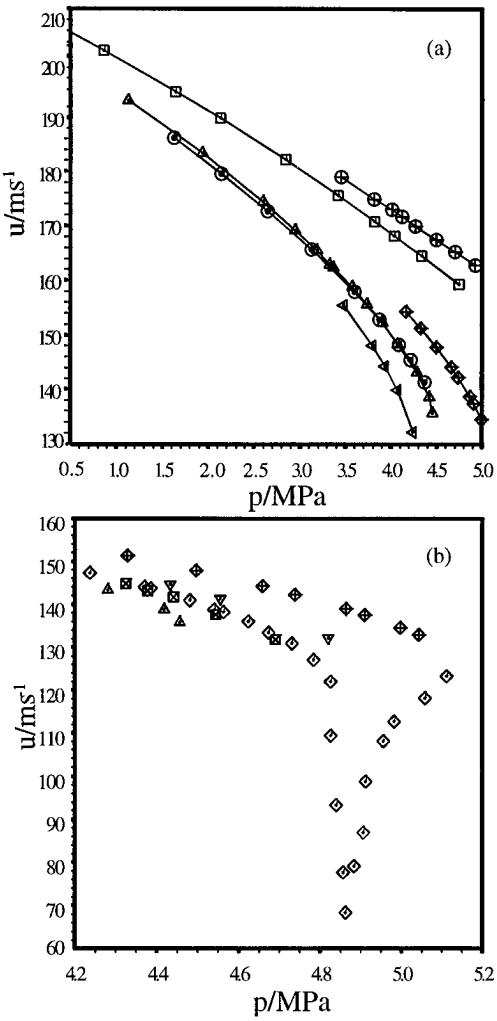

Figure 4. Speed of sound u in trifluoromethane as a function of pressure p: (a) to illustrate the behavior away from the critical point; (b) to illustrate the behavior close to the critical point; (dotted triangle pointing to the left) T = 294.07 K; (⊙) T = 296.85 K; (△) T = 298.15 K; (× inside square) T = 299.35 K; (dotted tilted square) T = 299.55 K; (dotted inverted triangle) T = 300.65 K; (+ inside tilted square) T = 302.99 K; (⊡) T = 313.18 K; (⊕) T = 318.17 K. Measurements have been made at nine different temperatures as indicated. In (a), the measurements have been joined with solid lines so that it is easier to distinguish between the different isotherms.

each resonance were represented by eq 1, to obtain estimates of the frequency (f_0) of the peak maximum and the peak half-width (g_0). Estimates of the uncertainties in f_0 and g_0 were given by the fitting routine. These ranged from 0.34 Hz for the fifth resonance to 0.02 Hz for the sixth. This is equivalent to an uncertainty of between (0.03 and 0.53) s^{-1} in $u/a \approx 4000$ s^{-1} for each resonance. For each peak, the measured half-width was reduced by an estimate of the losses due to vibrational relaxation, bulk thermal conductivity, and bulk viscosity. The vibrational relaxation time of trifluoromethane has been well studied (Cottrell and McCoubrey, 1961) and contributes between (0.2 and 3.6) s^{-1} to g_b. Experimental measurements of both the thermal conductivity (Makita et al., 1981) and the viscosity (Clifford et al., 1977) are available. Neither the thermal conductivity nor the viscosity is required with any great accuracy as their combined contribution to g_b is always less than 0.1 s^{-1}. u/a was obtained from the unweighted mean of the measurements.

The values of u_{exp}, the measured speed of sound, obtained at each temperature, are given in Table 3. Values of u_{exp}

Table 3. Experimental Results for the Determination of the Speed of Sound u in Trifluoromethane as a Function of Pressure p for Seven Different Isotherms[a]

T/K	p/MPa	u_{exp}[b]/ ms^{-1}	$(u_{exp} - u_{fit}$[c]$)$/ ms^{-1}	u_{calc}[d]/ ms^{-1}	$(u_{exp} - u_{calc})$/ ms^{-1}	T/K	p/MPa	u_{exp}[b]/ ms^{-1}	$(u_{exp} - u_{fit}$[c]$)$/ ms^{-1}	u_{calc}[d]/ ms^{-1}	$(u_{exp} - u_{calc})$/ ms^{-1}
294.072	4.241	132.24		138.22	−5.98	294.072	3.797	148.24	−0.07	150.33	−2.08
	4.003	139.94	−0.04	143.52	−3.58		3.480	155.56	0.01	156.82	−1.26
	3.937	144.42	0.10	147.07	−2.65						
				number of terms in u_{fit} 3, standard error of fit 0.12 ms^{-1}							
296.854	4.369	136.60		141.48	−4.87	296.854	3.123	165.37	0.01	165.87	−0.50
	4.214	141.84		145.53	−3.69		2.644	172.96	−0.00	172.91	0.05
	4.091	145.63	−0.01	148.38	−2.76		2.141	180.21	0.00	179.72	0.49
	3.871	150.95	0.02	152.98	−2.03		1.628	186.79	0.00	186.25	0.54
	3.598	156.70	−0.02	158.06	−1.36						
				number of terms in u_{fit} 5, standard error of fit 0.022 ms^{-1}							
298.126	4.456	135.80		142.12	−6.31	298.126	3.371	162.50	0.01	163.26	−0.76
	4.418	138.70		143.10	−4.40		3.186	165.69	−0.09	166.11	−0.41
	4.281	143.23		146.40	−3.16		2.950	169.41	−0.08	169.65	−0.18
	4.067	148.54	0.07	149.00	−2.45	298.150	3.326	163.07	0.20	163.98	−0.91
	3.906	152.35	−0.14	154.11	−1.76		2.592	174.56	0.02	174.59	−0.04
	3.736	155.72	0.02	157.20	−1.48		1.934	183.47	0.01	183.16	0.32
	3.569	158.98	−0.02	160.05	−1.07		1.129	193.17	−0.00	192.88	0.29
				number of terms in u_{fit} 5, standard error of fit 0.12 ms^{-1}							
299.322	4.691	131.77		138.69	−6.92	299.322	3.832	155.63	0.04	157.03	−1.41
	4.543	137.70		142.63	−4.94		3.626	159.32	−0.08	160.47	−1.16
	4.440	141.59	0.003	145.10	−3.51		3.498	161.61	−0.01	162.51	−0.90
	4.379	143.12	−0.10	146.47	−3.35		3.308	164.86	0.07	165.42	−0.56
	4.325	144.69	0.06	147.65	−2.96		3.118	167.86	−0.01	168.21	−0.35
	4.171	148.43	0.04	150.80	−2.36		2.957	170.49	−0.01	170.49	−0.00
	3.984	152.50	−0.03	154.35	−1.85						
				number of terms in u_{fit} 4, standard error of fit 0.067 ms^{-1}							
299.551	5.111	123.31		184.50		299.551	4.673	135.962		139.82	
	5.059	118.15		178.60			4.623	135.96	−0.024	141.16	−5.22
	4.981	112.61		167.96			4.563	138.13	0.011	142.66	−4.53
	4.955	108.10		163.56			4.544	138.78	0.004	143.14	−4.36
	4.912	98.70		154.14			4.480	140.85	0.051	144.65	−3.75
	4.906	86.95		152.39			4.385	143.62	0.016	146.77	−3.13
	4.882	79.04		141.03			4.371	144.01	−0.062	147.07	−3.13
	4.861	68.28		134.60			4.238	147.36	−0.021	149.84	−2.50
	4.857	77.64		134.65			4.134	149.70	0.0021	151.88	−2.16
	4.840	93.2		135.02			4.116	150.09	0.012	152.22	−2.12
	4.826	109.4		135.41			3.088	168.65	0.013	168.84	−0.19
	4.826	122.0		135.41			2.098	182.39	−0.001	181.93	0.47
	4.783	127.12		136.69			0.781	197.74	0.000	197.46	0.29
	4.731	130.97		139.82							
				number of terms in u_{fit} 6, standard error of fit 0.037 ms^{-1}							
300.650	4.989	142.11				300.650	4.556	141.25			
	4.820	132.20					4.433	144.59			
302.987	5.043	132.86	−0.02	140.04	−7.20	302.987	4.659	144.23	0.00	147.57	−3.33
	4.997	134.57	0.04	140.90	−6.29		4.497	147.88	0.02	150.56	−2.66
	4.909	137.50	−0.04	142.65	−5.19		4.328	151.38	−0.01	153.52	−2.16
	4.864	138.86	0.04	143.56	−4.65		4.164	154.46	0.00	156.24	−1.78
	4.738	142.30	−0.03	146.05	−3.81						
				number of terms in u_{fit} 5, standard error of fit 0.042 ms^{-1}							
313.176	4.747	159.35	0.02	161.05	−1.68	313.176	1.645	194.81	−0.00	194.11	0.69
	4.332	164.65	−0.02	165.85	−1.22		0.864	202.27	0.05	201.81	0.51
	4.036	168.36	−0.09	169.18	−0.90		0.433	206.37	0.00	206.01	0.36
	3.821	171.01	0.09	169.18	−0.90		0.279	207.86	−0.07	207.50	0.29
	3.419	175.84	0.04	175.92	−0.05		0.179	208.84	−0.05	208.46	0.32
	2.848	182.36	−0.04	181.93	0.39		0.134	209.28	0.00	208.91	0.38
	2.135	189.93	−0.01	189.21	0.70		0.109	209.53	0.08	209.14	0.15
				number of terms in u_{fit} 5, standard error of fit 0.063 ms^{-1}							
318.170	4.928	162.91	−0.03	164.74	−1.83	318.170	4.119	171.86	−0.05	172.77	−0.91
	4.701	165.37	0.04	167.00	−1.63		4.007	173.17	−0.13	173.88	−0.71
	4.499	167.61	0.02	169.00	−1.39		3.809	175.08	0.10	175.81	−0.73
	4.269	170.12	0.06	171.20	−1.08		3.450	179.06	−0.01	179.30	−0.24
				number of terms in u_{fit} 3, standard error of fit 0.085 ms^{-1}							

[a] The measured value of the speed of sound u_{exp} has been compared with the speed of sound u_{calc} calculated from a published equation of state (Hori et al., 1982). In addition, u_{exp} have been represented by Chebychev polynomials, and the difference between the smoothed values u_{fit} and the experimental values is also presented. [b] With $a = 0.04500$ m. [c] u_{fit} has been calculated from the best representation of the isotherm using Chebychev polynomials. [d] Using the equation of state published by Hori et al. (1982).

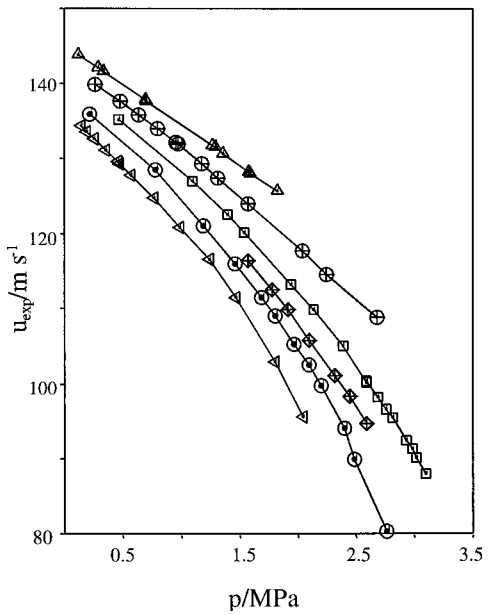

Figure 5. Speed of sound u in hexafluoroethane as a function of pressure p: (△) 321.52 K; (⊡) 300.00 K; (⊙) 290.10 K; (⊕) 312.11 K; (+ inside tilted square) 295.00 K; (dotted triangle pointing to the left) 281.90 K. Measurements have been made at six different temperatures as indicated. In the diagram, the measurements have been joined with solid lines so that it is easier to distinguish between the different isotherms.

were fitted to a Chebychev polynomial in powers of pressure; the deviations between u_{exp} and the value of the speed of sound predicted by the Chebychev polynomial u_{fit} are also given. Measurements within 95% of the vapour pressure, and within 0.2 MPa and 1 K of the critical point, were not included in this analysis. The standard deviations of the fits were about 0.03%, and in many cases they were better than this. The experimental results are illustrated in Figure 4. Figure 4a shows the results away from the critical region, and Figure 4b shows the behavior near the critical point. The precision of the measurements near the critical point is reduced due to experimental difficulty in assigning the observed resonances to specific modes of the resonator, and to an uncertainty in the magnitude of any critical dispersion.

As a final test of the quality of our measurements, we represented all of the measurements that we had represented by the Chebychev polynomials (a total of 56 points at 8 different temperatures) by two-dimensional Chebychev polynomials. It was found that a polynomial fifth order in T and third order in p gave a representation with a standard error of fit similar to that obtained for the individual isotherms (0.065 m s^{-1}). This again confirms that the precision of our measurements is about 0.05%.

5.2. Results for Hexafluoroethane. The individual results for hexafluoroethane are similar to those presented for trifluoromethane. Again, data required to calculate g_b were found in the literature (McCoubrey and Singh, 1960). Table 4 gives the values of u_{exp}, the measured speed of sound, obtained at each temperature. Values of u_{exp} were fitted to a Chebychev polynomial in powers of pressure; the deviations between u_{exp} and the value of the speed of sound predicted by the Chebychev polynomial u_{fit} are also given. The standard errors of all the fits were less than 0.1%. The experimental results are illustrated in Figure 5.

As a final test of the quality of our measurements, we represented all of the results (a total of 85 points at 6 different temperatures) by two-dimensional Chebychev polynomials. It was found that a polynomial fourth order in T and fifth order in p gave a representation with a standard error of fit similar to that obtained for the individual isotherms (0.117 m s^{-1}). This again confirms that the precision of our measurements in hexafluoroethane is about 0.1%.

6. Discussion

6.1. Trifluoromethane. Our measurements of the speed of sound can be divided into two regions: those well away from the critical point, which should be adequately described by analytical equations of state, and those close to the critical point. An accepted analytical equation of state for trifluoromethane has been developed by Hori et al. (1982). They propose that their equation is good to about 0.2% for pressures up to 11.6 MPa in the temperature range (203 to 383) K which has been confirmed by other researchers (Rubio et al., 1989; Rubio et al., 1991). Their comparison with heat capacity measurements is satisfactory, but there appears to be a discrepancy in a comparison with Joule-Thomson coefficients. A more recent equation of state (Rubio et al., 1989) has been optimized for a higher density region than covered in this work.

Using the equation of state proposed by Hori et al. (1982) and their correlation of the ideal gas heat capacity, it is possible to calculate the speed of sound u_{calc} of trifluoromethane at all of the temperatures and pressures covered in this work. These values are also tabulated in Table 3. The differences between our measured values of u_{exp} and u_{calc} are plotted in Figure 6. An uncertainty of 1% in the density of the fluid corresponds to an uncertainty of between (0.1 and 0.4) m s^{-1} in the speed of sound. This suggests that the uncertainty in the predicted speed of sound is about the same as the uncertainty in our measured speed of sound. Inspection of Figure 6 suggests that at pressures greater than 35 bar the differences between the predicted speed of sound and measured speed of sound become significant. At low temperatures this could be due to the approach to the two-phase region or to the critical point, but at 318 K, we are 20 K above the critical temperature and significant deviations still exist. However, we can conclude that there is substantial agreement between our results and the equation of state; improving the representation of the speeds of sound may well lead to a reduction in the ability of the equation to represent heat capacity measurements.

Our measurements near the critical point require very careful interpretation. The observed minimum is very pronounced, and satisfying. In addition, as shown in Figure 7, there is good agreement between the reduction in the speed of sound and the increase in the width of the resonance, indicating that we can observe the expected increase in the absorption of sound as the critical point is approached. However, due to the uncertainty in assigning the peaks in the spectra, the suggested speeds of sound are not unique. For this reason, we are aiming to produce more measurements in this region before any analysis is attempted. However, even in their "uncertain form" these results are an extension to the available measurements in the critical region of trifluoromethane (Aizpiri et al., 1991).

6.2. Hexafluoroethane. The amount of readily available thermophysical data on hexafluoroethane is suprisingly limited. In particular, the only proposed equation of state seems to come from a rough compilation using modified Soave−Redlich−Kwong parameters for a number of different fluorocarbons (Kadhem et al., 1989). There

Table 4. Experimental Results for the Determination of the Speed of Sound *u* in Hexafluoroethane as a Function of Pressure *p* at Seven Different Temperatures[a]

T/K	*p*/MPa	u_{exp}[b]/(ms^{-1})	$(u_{exp} - u_{fit}$[c]$)$/ms^{-1}	$(u_{exp} - u_{calcd})$/(ms^{-1})	*T*/K	*p*/MPa	u_{exp}[b]/(ms^{-1})	$(u_{exp} - u_{fit}$[c]$)$/ms^{-1}	$(u_{exp} - u_{calcd})$/(ms^{-1})
281.90	0.1452	134.38	−0.01	0.15	281.90	0.7642	124.75	−0.04	0.03
	0.1927	133.58	−0.05	0.04		0.9831	120.83	−0.21	−0.16
	0.2536	132.67	0.00	0.02		1.2358	116.48	0.11	0.09
	0.3525	131.16	0.02	−0.03		1.4654	111.48	−0.01	−0.35
	0.4561	129.59	0.06	−0.02		1.8045	102.92	0.03	−1.30
	0.4723	129.30	0.02	−0.07		2.0421	95.59	−0.02	−2.38
	0.5703	127.77	0.01	−0.06					
			number of terms in u_{fit} 4, standard error of fit 0.09 ms^{-1}						
290.10	0.2199	135.90	−0.01	0.64	290.10	1.9657	105.26	−0.19	−1.94
	0.7773	128.47	0.05	0.97		2.0929	102.51	0.06	−2.03
	1.1835	120.96	−0.14	−0.30		2.2005	99.73	0.01	−2.45
	1.4600	115.94	0.08	−0.72		2.398	94.04	0.00	−3.47
	1.6861	111.46	0.06	−1.16		2.485	89.86		−5.43
	1.8047	109.01	0.06	−1.37		2.766	80.35		−6.80
			number of terms in u_{fit} 5, standard error of fit 0.12 ms^{-1}						
295.00	1.5691	116.35	−0.02	−1.16	295.00	2.3178	101.04	−0.00	−3.25
	1.7766	112.45	0.02	−1.66		2.4432	98.29	0.12	−3.50
	1.9099	109.85	0.07	−1.97		2.5863	94.73	−0.06	−4.08
	2.0949	105.80	−0.13	−2.71					
			number of terms in u_{fit} 3, standard error of fit 0.10 ms^{-1}						
300.00	0.4619	135.18	−0.04	0.31	300.00	2.5884	100.32	−0.10	−3.67
	1.0963	126.96	0.14	0.20		2.6821	98.28	−0.04	−4.10
	1.3899	122.55	0.06	−0.18		2.7541	96.66	−0.00	−4.48
	1.5381	120.06	−0.12	−0.57		2.8121	95.52	0.23	−4.58
	1.9375	113.21	−0.20	−1.45		2.9327	92.47	0.10	−5.62
	2.1313	109.86	0.05	−1.75		2.9815	91.38	0.21	−5.92
	2.3865	105.02	−0.28	−2.41		3.0188	90.12	−0.10	−6.58
	2.5871	100.18	−0.27	−3.84		3.0995	87.95	−0.20	−7.56
			number of terms in u_{fit} 4, standard error of fit 0.18 ms^{-1}						
312.11	0.2654	139.89	0.04	−0.39	312.11	1.1727	129.31	0.02	−1.23
	0.4746	137.70	−0.01	−0.40		1.3082	127.41	−0.08	−1.61
	0.6312	135.84	−0.14	−0.60		1.5667	123.92	−0.05	−2.15
	0.7965	134.03	0.00	−0.64		2.0328	117.62	0.11	−3.01
	0.9542	132.16	0.06	−0.8−		2.2425	114.53	−0.09	−3.60
	0.9725	131.97	0.11	−0.78		2.6798	108.83	0.01	−4.14
			number of terms in u_{fit} 4, standard error of fit 0.09 ms^{-1}						
321.520	0.1188	143.90	−0.04	−0.03	321.52	1.2891	131.57	0.19	−1.32
	0.2900	142.11	−0.00	−0.25		1.3537	130.65	−0.03	−1.61
	0.3327	141.60	−0.04	−0.35		1.5778	128.23	−0.05	−1.86
	0.6935	137.90	0.13	−0.68		1.5903	127.97	−0.17	−1.99
	0.7000	137.65	−0.05	−0.87		1.8240	125.67	0.04	−2.01
	1.2600	131.73	0.04	−1.44					
			number of terms in u_{fit} 2, standard error of fit 0.10 m s^{-1}						

[a] u_{exp} values have been represented by Chebychev polynomials, and the difference between the smoothed values u_{fit} and the experimental values is also presented. [b] With $a = 0.04500$ m. [c] u_{fit} has been calculated from the best representation of the isotherm using Chebychev polynomials. [d] u_{calc} has been calculated from the modified Soave−Redlich−Kwong equation of state with the following parameters: $m = 0.7463$, $n = 0.1961$, $T^c = 293.01$ K, and $p^c = 3.04$ MPa.

have been some recent measurements on the vapor pressure (Kijima et al., 1977), and the critical parameters (Kijima et al., 1977; Wilson et al., 1995) appear to be well established. In addition there have been some recent measurements of the second virial coefficient (Bignall and Dunlop, 1993).

To obtain a comparison between our measurements and an equation of state, we chose to use the modified Soave−Redlich−Kwong equation of state (MSRK) (Soave, 1980). This equation of state has the form

$$p = RT/(V_m - b) - a(T)/[V_m(V_m + b)]$$

with

$$a(T) = a_c(1 - T/T^c)(m + nT^c/T)$$

m and n are adjustable parameters, and a_c and b are related to the critical parameters. Although this was optimized for polar substances, Kadhem et al. (1989) established that it represented the physical properties of hexafluoroethane better than the original Soave−Redlich−Kwong (SRK) equation of state (Soave, 1972). Obviously this equation of state will not predict our experimental measurements near the critical point (about 293 K and 3.1 MPa), but we might expect a reasonable representation at higher temperatures and lower pressures. The usual method of determining m and n is to choose the values that predict the vapor pressure curve with the greatest accuracy. Unfortunately, Kadhem et al. (1989) did not use the most recent values of the vapor pressure and the critical parameters, and so their suggested values of m and n ($m = 0.7321$, $n = -0.1971$) are not the best. Using the data of Kijima et al. (1989), we improved on the choice of m and

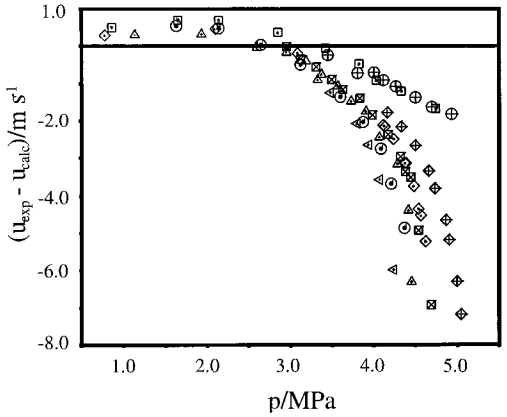

Figure 6. Difference ($u_{exp} - u_{calc}$) between the measured speed of sound in trifluoromethane and the speed of sound predicted by the accepted equation of state (Hori et al. 1982) as a function of pressure: (dotted triangle pointing to the left) $T = 294.07$ K; (⊙) $T = 296.85$ K; (△) $T = 298.15$ K; (× inside square) $T = 299.35$ K; (dotted tilted square) $T = 299.55$ K; (dotted inverted triangle) $T = 300.65$ K; (+ inside tilted square) $T = 302.99$ K; (⊡) $T = 313.18$ K; (⊕) $T = 318.17$ K.

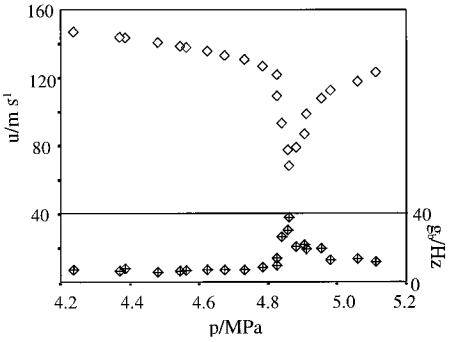

Figure 7. Behavior of the speed of sound in trifluoromethane at 299.551 K. Both the observed speed of sound u_{exp} and the corrected half-width of the resonance g_b at about 4 kHz are shown as a function of pressure. The maximum in the half-width appears to correspond to the minimum in the speed of sound.

n ($m = 0.7463$, $n = 0.1961$), leading to an improvement of 30% in the representation of the vapor pressure curve. These values of m and n were then used to calculate the speed of sound at the temperatures and pressures of our measurements. Throughout, the values of the critical parameters given by Kijima et al. (1977) were used. The calculated values of the speed of sound u_{calc} are given in Table 4, and the difference between the measured and the calculated speed of sound is illustrated in Figure 8. Inspection of these results shows that the MSRK equation of state in this form is very poor at predicting our experimental measurements. However, from this simplistic analysis, we have demonstrated that our experimental results do indeed add to the available knowledge about the equation of state of hexafluoroethane.

7. Conclusion

In this work we have presented experimental measurements to show that it is possible to measure the speed of sound in gases up to 5 MPa and under conditions approaching the two-phase region with an accuracy of better than 0.1%, using a simple annular resonator. We have shown that results of this accuracy are useful in establishing the nature of the equation of state of a fluid. When we embarked on this work, we hoped that we would achieve an accuracy better than we have actually achieved and that the resonator could be used to study the behavior of the speed of sound as the gas−liquid critical point is approached. We believe that, if this is to be achieved, we need to reduce the surface to volume ratio so that the losses at the walls of the resonator are reduced. Work is under way to achieve this goal.

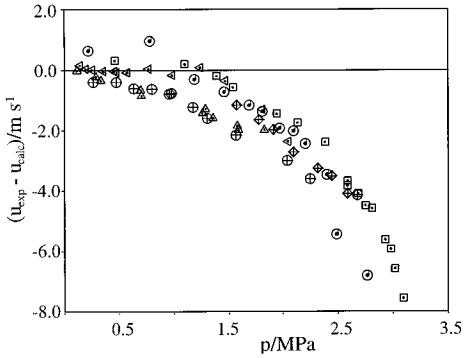

Figure 8. Difference ($u_{exp} - u_{calc}$) between the measured speed of sound in hexafluoroethane and the speed of sound predicted by the modified Soave−Redlich−Kwong equation of state (see the text for details): (△) 321.52 K; (⊡) 300.00 K; (⊙) 290.10 K; (⊕) 312.11 K; (+ inside tilted square) 295.00 K; (dotted triangle pointing to the left) 281.90 K.

Literature Cited

Aizpiri, A. G.; Rey, A.; Davilla, J.; Rubio, R. G.; Zollweg, J. A.; Streett, W. B. Experimental and theoretical study of the equation of State of CHF_3 in the Near-Critical Region. *J. Phys. Chem.* **1991**, *95*, 3351−3357.

Bignall, C. M.; Dunlop, P. J. 2nd Virial Coefficients for 7 Fluoroethanes and Interaction 2nd Virial Coefficients for their Binary Mixtures with Helium and Argon. *J. Chem. Phys.* **1993**, *98*, 4889−4891.

Clifford, A. A.; Gray, P.; Scott, A. C. Viscosities of $CFCl_3$, CF_3Cl, $CHFCl_2$, CHF_2Cl, and CHF_3 from 373 to 570 K. *J. Chem. Soc. Faraday Trans. 1* **1979**, 1752−1756.

Colgate, S. O.; Sivaraman, A.; Reed, K. Acoustic Determination of the Ideal-Gas Heat-Capacity of n-Heptane at high temperatures *J. Chem. Thermodyn.* **1990**, *22*, 245−252.

Colgate, S. O.; Sivaraman, A.; Dejsupa, C.; McGill, K. C. Acoustic Cavity Method for Phase-Boundary Determinations - The Critical Temperature of CO_2. *Rev. Sci. Instrum.* **1991a**, *62*, 198−202.

Colgate, S. O.; Sivaraman, A.; Dejsupa, C.; McGill, K. Acoustic-Resonance Determination of Sonic Speed and Dew Points in a Natural-Gas Mixture and Retrograde Condensate. *J. Chem. Thermodyn.* **1991b**, *23*, 647−652.

Cottrell, T. L.; McCoubrey, J. C. *Molecular Energy Transfer in Gases*; Butterworths: London, 1961; p 102.

Ewing, M. B.; McGlashan, M. L.; Trusler, J. P. M. The Temperature-Jump Effect and the Theory of the Thermal-Boundary Layer for a Spherical Resonator- Speeds of Sound in Argon at 273.16 K. *Metrologia* **1986,** *22*, 93−102.

Ewing, M. B.; Trusler, J. P. M. Speeds of Sound in CF_4 between 175 K and 300 K measured with a spherical resonator. *J. Chem. Phys.* **1989a**, *90*, 1106−1115.

Ewing, M. B.; Owusu, A. A.; Trusler, J. P. M. 2nd Acoustic Virial Coefficients of Argon between 100 and 304 K. *Physica A* **1989b**, *156*, 899−908.

Ewing, M. B.; Goodwin, A. R. H. An Apparatus based on a Spherical Resonator for Measuring the Speed of Sound in Gases at High Pressures. Results for Argon at Temperatures between 255 K and 300 K and at Pressures up to 7 MPa *J. Chem. Thermodyn.* **1992**, *24*, 531−547.

Garland, C. W.; Williams, R. D. Low Frequency Sound Velocity near the Critical Point of Xenon. *Phys. Rev. A* **1974**, *10*, 1328−1332

Hori, K.; Okazaki, S.; Uematsu, M.; Watanabe, K. An Experimental Study of Thermodynamic Properties of Trifluoromethane. *In Proceedings of the 8th Symposium on Thermophysical Properties*; Sengers, J. V., Ed: Amerciam Society of Mechanical Engineers: New York, 1982; Vol. 8, pp 380−386.

Kadhem, G. M. A.; Al-Sahaf, T. A.; Hamen, S. E. M. Parameters of the modified Soave-Redlich-Kwong equation of state for some Chlorofluorocarbons, Hydrofluorocarbons, and Fluorocarbons. *J. Fluorine Chem.* **1989**, *43*, 87−104.

Kijima, J.; Saikawa, K.; Watanabe, K. Experimental Study of Thermodynamic Properties of Hexafluoroethane (R116). *Proc. Symp. Thermophys. Prop.* **1977**, 480−488.

Makita, T.; Tanaka, Y.; Morimoto, Y.; Noguchi, M.; Kubota, H. Thermal Conductivity of Gaseous Fluorocarbon Refrigerants R21, R13, R22, and R23, under Pressure. *Int. J. Thermophys.* **1981**, 3, 249−268.

McCoubrey, J. C.; Singh, Narinder Mohan The Viscosity of some Fluorocarbons in the Vapour Phase. *Trans. Faraday Soc.* **1960**, *56*, 486−489.

Mehl, J. B.; Moldover, M. R. Precision Acoustic Measurements with a Spherical Resonator - Ar and C_2H_4. *J. Chem. Phys.* **1981**, *74*, 4062−4077.

Moldover, M. R.; Trusler, J. P. M.; Edwards, T. R.; Mehl, J. B.; Davis, R. S. Measurement of the Universal Gas-Constant R using a Spherical Acoustic Resonator. *J. Res. Natl. Bur. Std. (U.S.)* **1988**, *93*, 85−144.

Morse, P. M.; Ingard, K. U. *Theoretical Acoustics*; McGraw-Hill: New York, 1968; p 603.

Rubio, R. G.; Zollweg, J. A.; Streett, W. B. A p-V-T Surface for Trifluoromethane. *Ber. Bunsen-Ges. Phys. Chem.* **1989**, *93*, 791−800.

Rubio, R. G.; Zollweg, J. A.; Palanco, J. M. G.; Calado, J. C. G.; Miller, J.; Streett, W. B. Thermodynamic Properties of Simple Molecular Fluids: Tetrafluoromethane and Trifluoromethane. *J. Chem. Eng. Data* **1991**, *36*, 171−184.

Soave, G., Equilibrium Constants from a Modified Redlich Kwong Equation of State. *Chem. Eng. Sci.* **1972**, *27*, 1197−1203.

Soave, G. Rigorous and Simplified Procedures for determining the Pure-component Parameters in the Redlich-Kwong-Soave Equation of State. *Chem. Eng. Sci.* **1980**, *35*, 1725−1729.

Trusler, J. P. M.; Zarari, M. The Speed of Sound and Derived Thermodynamic Properties of methane at Temperatures between 275 K and 375 K and Pressures up to 10 MPa. *J. Chem. Thermodyn.* **1992**, *24*, 973−991

Trusler, J. P. M. The Speed of sound in $(0.8\ CH_4 + 0.2C_2H_6)$(g) at temperatures between 200 K and 375 K and amount -of-substance densities up to 5 mol dm^{-3}. *J. Chem. Thermodyn.* **1994**, *26*, 751−763.

Received for review September 12, 1995. Accepted November 11, 1995.[⊗]

JE950231Z

[⊗] Abstract published in *Advance ACS Abstracts*, January 15, 1996.